Aggregation Phenomena in Aqueous Solutions of Uncharged Star Polymers with a Porphyrin Core

ARTICLE *in* THE JOURNAL OF PHYSICAL CHEMISTRY B · MAY 2003

Impact Factor: 3.3 · DOI: 10.1021/jp026999p

9 AUTHORS, INCLUDING:

Placido Mineo
University of Catania
92 PUBLICATIONS **1,309** CITATIONS
SEE PROFILE

Vincenza Crupi
Università degli Studi di Messina
162 PUBLICATIONS **1,622** CITATIONS
SEE PROFILE

Valentina Venuti
Università degli Studi di Messina
137 PUBLICATIONS **1,444** CITATIONS
SEE PROFILE

Aggregation Phenomena in Aqueous Solutions of Uncharged Star Polymers with a Porphyrin Core

Norberto Micali and Valentina Villari

Istituto per i Processi Chimico-Fisici del CNR, Sezione di Messina, Via La Farina 237, I-98123 Messina, Italy

Placido Mineo and Daniele Vitalini

Istituto per la Chimica e la Tecnologia dei Materiali Polimerici CNR, Viale Andrea Doria 6, I-95125 Catania, Italy

Emilio Scamporrino

Dipartimento di Scienze Chimiche, Universita' di Catania, Viale Andrea Doria 6, I-95125 Catania, Italy

Vincenza Crupi, Domenico Majolino, Placido Migliardo,* and Valentina Venuti

Dipartimento di Fisica and INFM Unita' di Messina, Universita' di Messina, C.da Papardo S.ta Sperone 31, P.O. Box 55, I-98166, Messina, Italy

Received: September 16, 2002; In Final Form: January 24, 2003

Uncharged star polymers having a porphyrin core and four poly(ethylene glycol)methyl ether (PEGME) arms have been synthesized and investigated (through the study of the structural and dynamical properties) as a function of the molecular mass of the arms, in different thermodynamic conditions. Molecules with short PEGME arms are insoluble in water, whereas in the presence of long PEGME chains, the star polymers are water-soluble; for the intermediate length of the arms, the building up of large rigid monodisperse aggregates, driven by the diffusion limit aggregation mechanism, has been observed by means of static and dynamic light scattering. These aggregated systems, whose sizes are modulated by changing the pH and triggered by the chain flexibility, can be well described in terms of the DLVO interparticle potential in the frame of the colloidal theory.

I. Introduction

The growing interest in the study of the static and dynamic properties of star-polymer solutions can be traced back to the fact that, thanks to their peculiar architecture, their physical properties can change from those of polymers to those of colloids.[1−3] In particular, the variation of the functionality (the number of the arms),[4,5] the length of the arms, and the solvent affinity affect the conformation of a single star and the interactions with the other stars, giving rise to different phase diagrams and ordering phenomena.[6] On the other hand, although the core of the star is usually small, compared with the overall extension of the whole molecule, the thermodynamic properties of the solution (and hence its stability) as well as the intermolecular interactions can depend on the chemical−physics features of the cores.

With the term "star" or "star-like", a wide class of molecules is involved; they consist of linear polymer chains grafted to one common central core, which can be a polyfunctional unit or a dentritic precursor. Also comb polymers at high molecular mass, with amphoteric nature can assume a starlike conformation.[7]

The present work reports on the static and dynamic properties of aqueous solutions of uncharged water-soluble star polymers, having a porphyrin core and four poly(ethylene glycol) methoxy terminated arms, and on the effect of the length of the arms on the aggregation phenomena.

* To whom correspondence should be addressed. E-mail: migliard@dsme01.unime.it.

These star polymers represent a model of water-soluble multibranched materials, whose amphiphilic character depends on the hydrophobic/hydrophilic balance between the porphyrin core and the PEGME branches. It will be shown that the aggregation of the molecules, driven by the porphyrin cores, can be piloted varying the thermodynamic parameters of the solution.

Water-soluble porphyrins and their metal derivatives have recently been used in some biological fields such as in the inhibition of protease-resistant prion protein (PrP-res) formation (critical in the transmissible spongiform encephalopathies (TSE) pathogenesis)[8,9] or in the chemotherapy for their strong affinity toward cancer cells.[10,11]

Most studies on these fields have been made by using cationic or anionic porphyrins, and only a few works have appeared in the literature about uncharged molecules; however, although the affinity to DNA of these porphyrin derivatives seems only slightly affected by electric charges, their interaction with cell membranes could be different.[12] Under these circumstances, these uncharged star polymers represent an interesting model to be studied.

Through the present study, we found that increasing the length of the PEGME arms improves the solubility of the molecules in water and obstructs the porphyrin cores stacking aggregation phenomena. Such aggregation takes place spontaneously in the sample having an average molecular mass ($\overline{M}_n$) of 2100 Da, giving rise to large fractal structures, whereas it can be induced in the star polymers at higher $\overline{M}_n$ values varying the thermodynamic parameters of the solution.

10.1021/jp026999p CCC: $25.00
Published on Web 04/26/2003

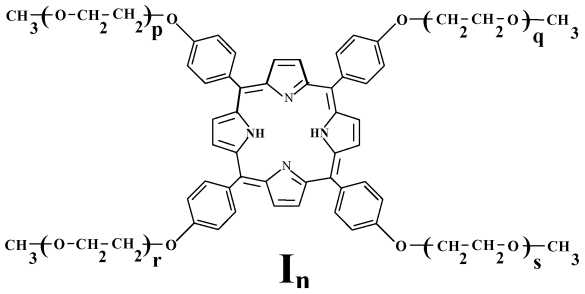

Figure 1. Structure of star polymers with porphyrin core and PEGME arms.

II. Experimental Details

Synthesis. Star polymers I_n (with $n = p + q + r + s$, see Figure 1) having an average molecular mass of 2100 ($\bar{n} \sim 31$), 3600 ($\bar{n} \sim 65$), and 8500 ($\bar{n} \sim 176$) Da, with a very narrow polydispersity ($M_w/M_n = 1.01$), were prepared by reaction between tetrakis(*p*-hydroxyphenyl) porphyrine (obtained from pyrrole and *p*-acetoxybenzaldheyde in boiling propionic acid)[13] and different chlorinated poly(ethylene glycol)methyl ethers (PEGMEC, formed by reaction of poly(ethylene glycol)methyl ether with thionyl chloride in THF).

As an example, the synthesis of the star polymer 2100 is reported here. In a 10 mL flask, 0.5 g of PEGMEC-350 (about 1.43 mmol) were dissolved in 6 mL of a H_2O/THF (1/1) solution; after the addition of 0.12 g of tetrakis(p-hydroxyphenyl)-porphyrin (0.177 mmol, half of the stoichiometric required quantity) dissolved in 1.42 mL of a 0.5 M NaOH aqueous solution, the mixture was refluxed 24 h (during this time, the color of the solution changes from green to purple as the pH goes toward neutrality). Then, 1.42 mL of 0.5 M NaOH and 1.5 mL of THF were further on added and the solution continuously refluxed. After 24 h, the reaction was stopped by the addition of CH_3COOH, the product was dried under vacuum, and the residue, dissolved in CH_3COCH_3, was fractionated by column chromatography using silica gel as stationary phase and a solution of $CHCl_3/C_2H_5OH/N(C_2H_5)_3$ (97/2/1) as eluant. Some fractions, constituted of porphyrin derivatives with a different number of polyethylenoxy branches, are recovered. For all of the synthesized star polymers, the yield of the tetra-branched fraction was about 30% with respect to the initial porphyrin amount.

Mass Spectrometric Analysis. The MALDI-TOF mass spectra were acquired by a Voyager DE-STR (PerSeptive Biosystem) using a simultaneous delay extraction procedure (20 kV applied after 233 ns with a potential gradient of 2545 V/mm and a wire voltage of 200 V) and detection in reflection mode. The instrument was equipped with a nitrogen laser (emission at 337 nm for 3 ns) and a flash AD converter (time base 2 ns). In each MALDI experiment, the specimen was prepared by loading about 50 pmol of product and 80 mmol of matrix (*trans*-3-indoleacrylic acid) on the sample plate, using THF as a solvent. The average molecular masses of the SP samples were determined using the Grams/386 program (by PerSeptive Biosystem) applied on spectra corrected for the offset and the baseline according to our method.[14]

Positive electrospray mass spectra were acquired on a Mariner ESI-TOF mass spectrometer (PerSeptive Biosystems) equipped with an API ion source. The ionspray voltage was fixed at 5 kV, and the orifice potential (declustering potential) was of 150 V. The aqueous solutions of the investigated samples, mixed with a CH_3OH/H_2O (60/40) mixture (the solute concentration was maintained at about 10^{-4} M in each experiment), were introduced into the source at a flow rate of 7 μL/min. The mass spectra were elaborated with the "BioSpec Data Explorer ver. 3.0.0.1" software (from PerSeptive Biosystems).

Static Light Scattering. Static light scattering (SLS) measurements were performed by using a computerized homemade goniometer and the 532 nm line of a duplicate Nd:YAG laser as exciting source. The investigated scattering angle range was $20° \le \theta \le 150°$ corresponding to exchanged wave vector values $5.5 \le k \le 30.5\ \mu m^{-1}$ (with $k = [(4\pi n)/\lambda]\sin(\theta/2)$, where n is the refractive index of the sample and λ is the vacuum incident wavelength). The integration time for each angle was 5 s. The measured scattered intensity of the solution was then normalized by the scattered intensity of toluene used as reference.

Small Angle Light Scattering. Small angle light scattering (SALS) was performed by means of a homemade standard apparatus using an optical Fourier transform and a HeNe laser ($\lambda = 633$ nm). A Fourier lens having a focal length of 100 mm focuses the low angle scattered light on the detector; this is a fiber linked 1024 channels diode 1 in. wide. This configuration allows for a k range from 0.99 to 2.8 μm^{-1}.

Quasielastic Light Scattering. Quasielastic light scattering (QELS) measurements were carried out by using the same apparatus as in SLS. The scattered light was collected, in a self-beating mode, through an optic fiber, by a cooled Hamamatsu R943−02 photo multiplier in single photon counting mode and sent to a Malvern 4700 particle analyzer. The correlator built up the intensity autocorrelation function in the time domain ranging from 10 μs to 1 s.

The temperature in light scattering experiment was fixed at 295 ± 0.01 K.

III. Data Analysis

A. Mass Spectrometry Characterization. All of the star polymers have been characterized by means of different techniques (mass spectrometry, ^1H and ^{13}C NMR, and GPC) to determine both the structure and the molecular mass.[15] The MALDI-TOF mass spectrum of star polymer 2100 is reported as an example in Figure 2a; three series of peaks are present in the spectrum at m/z values of $735 + n44.03$ (×, with $n = 19-40$, first peak in the spectrum at m/z 1571), $757 + n44.03$ (●, with $n = 20-41$, first peak in the spectrum at m/z 1637), and $773 + n44.03$ (*, with $n = 23-38$, first peak in the spectrum at m/z 1785), corresponding to I_n oligomers cationized with H^+, Na^+, or K^+, respectively. In Figure 2b, the ESI mass spectrum of star polymer 2100 is also reported; contrary to the MALDI case, in this spectrum, peaks corresponding to single charged ions are present with very low intensities at m/z values between about 1700 and 2300, whereas going toward lower masses, the presence of three intense envelopes, due to double, triple, and quadruple charged species, can be seen. Besides, different than the MALDI-TOF case, because of the high resolution of the ESI mass spectrometer, a cluster of isotopic peaks is recorded for each species detected, and in the following, the mass value of the first peak of each cluster will be reported. Considering the envelope corresponding to the double charge zone, a particular of which is reported in the inset of Figure 1b, different families of clusters can be seen, due to star polymer oligomers cationized by different combinations of H^+, Na^+, and K^+. So, as an example, the compound I_{27} ($M_w = 1923.0$ Da) containing complessively 27 ($-CH_2-CH_2-O-$) units in the four branches of the molecule, peaks at m/z 962.5, 973.5, 981.5, 984.5, 992.5, and 1000.5, corresponding to species cationized by $2H^+$, H^+-Na^+, H^+K^+, $2Na^+$, Na^+K^+, and $2K^+$, respectively, are found; the cluster due to I_{27} cationized by two Na^+ ions (cluster at m/z 984.5) is overlapped with that of the I_{28} cationized by two H^+

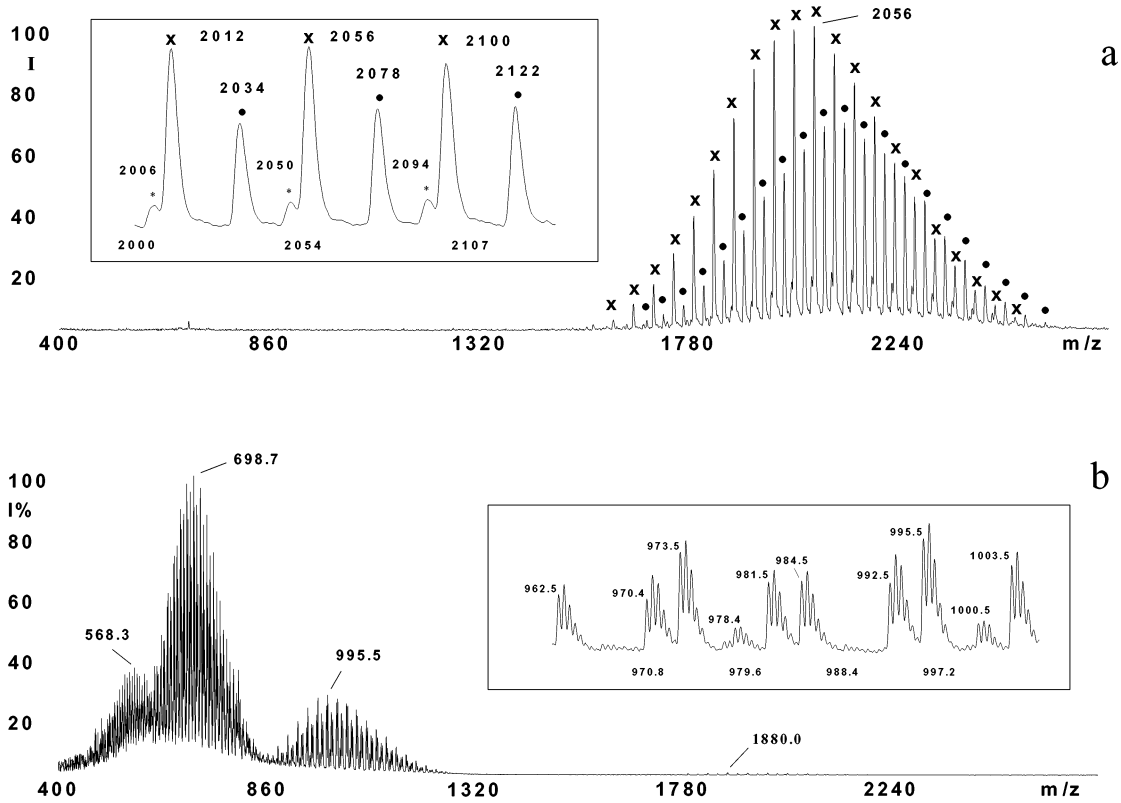

Figure 2. Mass spectrum of star polymer 2100 with (a) the MALDI-TOF technique and (b) the ESI technique.

ions and indistinguishable from the latter. The others clusters present in the inset are due to I_{26} cationized with Na^+K^+ and $2K^+$ (clusters at *m*/*z* 970.4 and 978.4) and I_{28} cationized with $2H^+$, H^+Na^+, and H^+K^+ (clusters at *m*/*z* 984.5, 995.5, and 1003.5), respectively. Considering the four envelopes, it can be noticed that the more intense peak found in each of them is due to $I_{26}H^+$ (*m*/*z* 1880.0) for the single charge zone, $I_{28}HNa^{2+}$ (*m*/*z* 1991.0/2) for the double charge zone, $I_{30}H_2K^{3+}$ or, more probably, $I_{29}Na_2K^{3+}$ (*m*/*z* 2096.0/3) for the triple charge zone, and $I_{34}H_3K^{4+}$ or, more probably, $I_{33}HNa_2K^{4+}$ (*m*/*z* 2273.1/4) for the quadruple charge zone; it follows that, with the increasing of the number of charges present on each molecule, higher molecular mass cationizing species are preferred (from H^+ for single charged species to HNa_2K^{4+} for quadruple charged ones), and the ionization efficiency is better for higher molecular mass species (the more intense peak in each envelope moves from I_{26} for single charged species to I_{33} for the quadruple charged ones).

B. Spectroscopic Characterization. By SLS at large and small angles, the scattered intensity profile of the solution, $I(k) \propto P(k)S(k)$, can be determined;[16] $P(k)$ and $S(k)$ (the form and the structure factor, respectively) allow the study of the conformational and structural properties of molecules in solution. However, for the wavelength involved in a light scattering experiment, the exchanged wave vector values are small enough that $P(k)$ is close to unity.[16] Depending on the aggregate size and choosing wave vector values low enough (SALS), the intensity $I(k)$ obeys a Gaussian law, known as Guinier law[16]

$$I(k) = \exp[-(1/3)(kR_g)^2] \tag{1}$$

R_g being the gyration radius (close to the aggregate size l_{max}). For k values such $kl_{min} \gg 1$ (l_{min} being building blocks size), the Porod limit gives $I(k) \propto k^{-4}$. For k values such as $kl_{max} \gg 1$ and $kl_{min} \ll 1$, the scattering intensity is model dependent. For example, the Ornestein−Zernike form $I(k) \approx (1 + \xi^2k^2)^{-1}$ can be suitable for describing the correlation length, ξ, of the density concentration fluctuations inside aggregates. For ideal mass fractals system (where the spatial correlation density fluctuation is an homogeneous function), the scattering intensity (spatial Fourier Transform of the correlation function) must obey a power law. For mass fractals it holds

$$S(k) \approx k^{-D_f} \tag{2}$$

where D_f is the fractal dimension of the aggregate.[17−20] For the finite fractal system, the power law behavior of the scattering intensity disappears for low k values, where the Guinier limit starts. A fit law in the k range encompassing the Gaussian and the fractal behavior of the structure factor was deduced by Chen and Teixeira.[21] For a fractal aggregate of m monomers is

$$S(k) = \frac{m \sin[(D_f - 1)\arctan(kR)]}{(D_f - 1)kR(1 + k^2R^2)^{(D_f-1)/2}} \tag{3}$$

where R is the radius of the aggregate, namely the cutoff parameter of the density correlation function of the fractal.[17,18]

Photon correlation spectroscopy (PCS) technique gives complementary information, allowing the investigation on the dynamics of aggregates themselves. It allows measurement of the normalized time autocorrelation function of the scattered intensity $I_S(k, t)$[16,22−24]

$$g_2(k, t) = \frac{\langle I_S(k, 0)I_S(k, t)\rangle}{\langle I_S(0)\rangle^2} \tag{4}$$

As it is well-known,[16] if the scattered field obeys the Gaussian statistics, the Siegert's relationship can be applied

$$g_2(k, t) = 1 + \alpha|g_1(k, t)|^2 \quad (5)$$

where α is a constant which depends on the experimental setup and $g_1(k, t)$ is the normalized field autocorrelation function. In the time domain typical for a light scattering experiment and for diffusing monodisperse spherical scatterers, the intensity correlation function decays exponentially, according to

$$g_2(t) = 1 + \alpha \exp(-2\Gamma t) \quad (6)$$

Generally, this quantity contains information on the translation dynamics and, consequently, on the hydrodynamic radius and on the anisotropy of the aggregates. In fact, for homogeneous, Euclidean, noninteracting monodisperse spheres, for $kR_g \ll 1$, it holds $\Gamma = D_c k^2$, where D_c is the collective translation diffusion coefficient.

D_c directly gives information on the hydrodynamic radius (that is an "effective" size, depending on the hydrodynamic interaction with the solvent and on the interparticle interactions) through the Einstein-Stokes relation $R_H = k_B T/(6\pi\eta D_c)$, with η the solvent viscosity and k_B the Boltzmann constant.[16]

In the opposite case, light scattering is sensitive to particle internal motions, and the simple k^2 dependence of the relaxation rate Γ loses validity. However, if the diffusing object is rigid and monodisperse, the k^2 dependence and the Einstein−Stokes relation are fulfilled as well.[16] In the case of moderately anysotropic scatterers (which happens in the case of fractals), the Einstein−Stokes relation is not suitable anymore leading to underestimate the value of R_H. For correctly evaluating R_H, therefore, it is necessary to use relations which take into account porosity and anysotropy of the object through proper parameters.[25]

Even in dilute solution, however, charged particles cannot be considered noninteracting and structural, and dynamical properties are affected by the strength of the interparticle potential. For charged colloidal particles, these interactions can be well described by the well-known Derjaguin−Landau−Verwey−Overbeek theory (DLVO),[26−28] which also accurately describes proper conditions for stability against aggregation as well as the kinetic mechanism driving aggregation phenomena. According to the DLVO potential, the interaction strength can be modulated controlling and adjusting the thermodynamic parameters of the system such as temperature, ionic strength, pH, particle volume fraction, etc.

The DLVO potential, $V(r)$, is related to the presence of a diffuse double layer surrounding the particles and results from the sum of a long-range repulsive shielded ionic interaction $V_R(r)$ and an attractive short-range van der Waals-London interaction $V_A(r)$ (r is the distance between the centers of the particles). The attractive part is $V_A(r) = -A/12\ [1/r_0^2 - 1 + 1/r_0^2 + 2ln(1 - 1/r_0^2)]$, where A is the Hamamaker constant depending on the interparticle, the solvent−solvent and the particle−solvent interactions.[29] If the radius of the particles, R_0, satisfies the condition $R_0 L \gg 1$ (with $L = (2e^2 N 10^3/\epsilon k_B T\ I)^{1/2}$ being the Debye screening length, e the electron charge, N the Avogadro number, and I the ionic strength), it follows that the repulsive part is $V_R(r) = 2\pi R_0 \epsilon \psi_0^2 \ln(1 + \exp[-2LR_0(r_0 - 1)])$, with ϵ the dielectric constant of the solvent and ψ_0 the particle surface potential. In the opposite case, $R_0 L \ll 1$, it holds $V_R(r) = 4\pi(R_0\psi_0)^2\epsilon/r \exp[-2LR_0(r_0 - 1)]$, where $r_0 = r/2R_0$.

The DLVO potential $V(r)$ described above exhibits two minima divided by a barrier, whose height depends on particle size and ionic strength. The existence of two minima determines the stable and metastable states and, therefore, the possibility of irreversible and reversible aggregation, respectively.[28] Increasing the ionic strength, for example, causes a decrease of the barrier height and a shortening of the lifetime of the metastable state.[30] For a low or null charge system, the aggregation phenomena are more evident, and an increasing of the charge destroys or reduces the size of the aggregation.

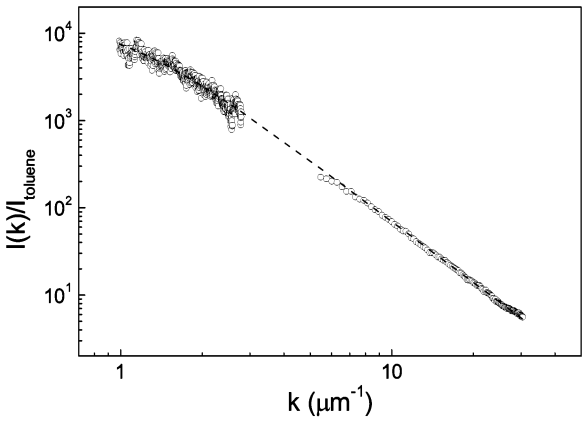

Figure 3. Scattered intensity profile, as referred to toluene, of the star polymer 2100 water solution at a concentration of 10^{-5} M. The dashed curve is the fit according to relation 3.

Therefore, by varying the overall particle charge or increasing the electrolyte concentration, it is possible to modulate the final aggregate properties and to separate the regions where colloids undergo reversible or irreversible aggregation. The structural and dynamical properties of these colloids can be directly observed by elastic and quasielastic light scattering.

IV. Results and Discussion

The aqueous solutions of star polymers at different molecular mass values present, for the species having molecular mass higher than 3000 Da, at least up to a concentration value of 10^{-4} M, a very low scattered intensity compatible with the presence of the molecules in the monomer form. On the other hand, the star polymer 2100 aggregates to form large supramolecular structures. Figure 3 shows that the scattered intensity of the latter sample is quite large, and the profile, as a function of the exchanged wave vector, obeys a power law in the range $2 \div 30\ \mu m^{-1}$, bending at smaller k values. To adopt the Chen and Teixeira structure factor, the two sets of data from a different experimental setup (referring to low and large scattering angles) were matched introducing a multiplicative factor as a free parameter in the fit relation 3. As it can be seen in Figure 3, the agreement between data and fit is very good and indicates that the aggregates arrange in a fractal structure having a fractal dimension $D_f = 2.3 \pm 0.1$ and have a radius of $0.9 \pm 0.05\ \mu m$. The corresponding gyration radius is $R_g = (D_f/(2 + D_f)\ R^2)^{0.5} \simeq 0.6\ \mu m$.[31] The fractal dimension alone, however, may not suffice to uniquely characterize the morphology of random aggregates and must be compared with the information obtained from the dynamics. As far as the dynamic properties of these aggregates are concerned, a single exponential can fit the correlation functions. The comparison with the results obtained using a cumulant expansion shows that the variance is less than 0.1, indicating that the aggregates display a low polydispersity. The k^2 dependence of the decay rate, Γ, of the intensity autocorrelation function (shown in Figure 4) suggests that the relaxation process, occurring at the microsecond time scale, is diffusive even if $kR_g \gg 1$, typical of monodisperse rigid clusters; the obtained D_c is $1.1 \pm 0.1 \times 10^{-8}$ cm^2/s.

The experimentally obtained fractal dimension, together with the fact that the aggregates are monodisperse, suggests that the

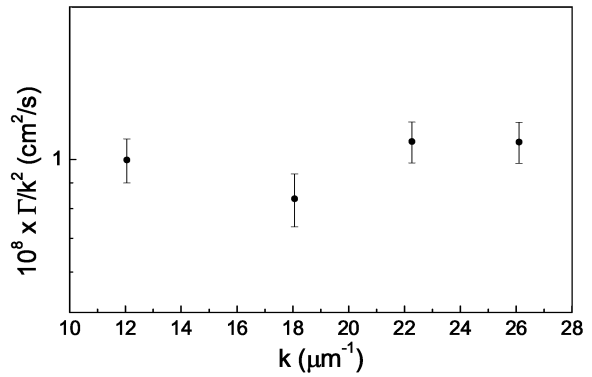

Figure 4. Γ/k^2 as a function of k for the star polymer 2100 water solution at a concentration of 10^{-5} M. Its k independence suggests a diffusive motion of the aggregates.

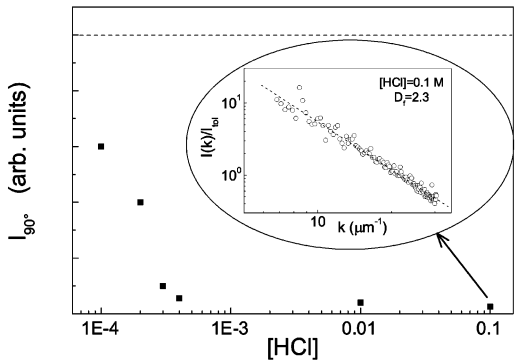

Figure 5. Scattered intensity as a function of HCl concentration. The dashed line at the top of the figure indicates the intensity scattered from the sample without HCl. In the inset, the scattered intensity profile referred to toluene of the star polymer 2100 water solution at a concentration of 10^{-5} M at [HCl] = 10^{-1} M. The dashed curve is the fit according to relation 2.

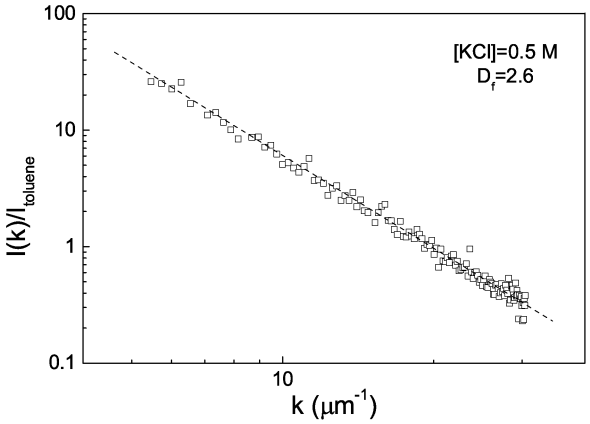

Figure 6. Scattered intensity profile referred to toluene of the star polymer 3600 water solution at a concentration of 10^{-5} M with the addition of 0.5 M of KCl. The dashed curve is the fit according to relation 2.

aggregation is driven by a diffusion-limited aggregation (DLA) mechanism (theoretical calculations provides for a value of 2.5).[17,18] Although the fractal dimension found for star polymer 2100 is slightly lower than the theoretical value, previous results on other porphyrin aggregates[32−34] indicated that the aggregation is driven by a DLA mechanism.

The building up of DLA fractals from the stacking process of porphyrin cores is generally preceded by a reaction limited aggregation (RLA) mechanism. As highlighted in reference 32, in fact, there exists a crossover from a RLA early stage to the final DLA aggregation kinetics, giving rise to more isotropic objects.

Using the Einstein−Stokes formula, we obtain, for the hydrodynamic radius, the value $R_H \simeq 0.19$ μm. As a matter of fact, this value refers to the hydrodynamic radius of an isotropic, homogeneous sphere. Because of the fact that the investigated system is a fractal, it is slightly anysotropic;[33,35,36] as a consequence, we expect that the hydrodynamic radius evaluated from the Einstein−Stokes relation is underestimated. To estimate more correctly R_H for such aggregates, the following form is more suitable:[25]

$$\Gamma(k) = k^2 D\left(1 + \frac{\alpha^2}{4\beta^2}\right) \tag{7}$$

where $\beta = R_H/R_g$ is a measure of the porosity of a cluster and α is directly related to its anisotropy. In other words, when $kR_g \gg 1$, the light scattering experiment is sensitive to the effect of rotations and the "effective" diffusion coefficient rises to a higher limit depending on the ratio β. Taking into account that, in the case of fractals with an exponential cutoff in the density correlation function, $\beta = 0.62$[37,38] and $\alpha = 1.5$ (for colloidal systems), from the R_g value obtained by the fit of the Static measurements, we extract $R_H \simeq 0.37$ μm.

At their natural pH, these star polymers are uncharged, and spontaneous fractal aggregates are formed. To understand if the system displays colloidal properties, the solution of star polymer 2100 was perturbed introducing an increasing amount of hydrochloric acid. The measured scattered intensity at $\theta = 90°$ clearly decreases adding HCl, as shown in Figure 5.

The effect of adding hydrochloric acid consists of the fact that porphyrin cores are protonated by H^+ ions (which link to nitrogen atoms lone pairs) so that molecules take a positive charge. The strong electrostatic repulsion makes molecules repel one another and forces the aggregate to break up. In fact, at high HCl concentration values, the low scattered intensity (about 10 times lower) indicates that smaller entities are present. However, the absolute scattered intensity profile at [HCl] = 10^{-1}M, shown in the inset of Figure 5, suggests that the aggregates, despite their smaller size, still have a fractal arrangement with the same fractal dimension as the sample without HCl.

The experimental evidence of aggregation phenomena only at the intermediate molecular mass, as in the case of star polymer 2100 for which the polymerization degree of PEGME branches is ≃8 (shorter PEGME chains do not favor solubility in water), suggests that longer PEGME chains obstruct porphyrins to approach one another and avoid that the stacking interactions responsible for aggregation take place.

The possibility of inducing aggregation modifying the thermodynamic parameters of a solution is a typical behavior of colloidal state.

For the star polymer 3600 case, whose molecules in solution appear as separate species (up to 10^{-4} M), the addition of KCl (up to obtain a 0.5 M solution) induces an aggregation effect; in fact, the scattered intensity at $\theta = 90°$ rapidly increases and the wave vector profile (Figure 6) changes from a flat behavior without salt to a power law dependence in the presence of KCl.

This occurrence could be ascribed to different mechanisms: (a) The ability of polar PEG arms of coordinating K^+ ions allows the uncoiling of the chains;[39,40] in this way, the unscreened porphyrin rings can more easily form aggregates by stacking one another. (b) The decrease of PEGME solubility in water; in this case the aggregation would be driven by both the

porphyrin−porphyrin attraction and the interaction between polymer chains.

The results here reported suggest that the investigated star-polymer solutions can be inserted in the frame of colloidal theory and their properties can be described in terms of the DLVO interparticle potential.

V. Concluding Remarks

The family of uncharged star polymers having a porphyrin core, synthesized in our laboratory with different lengths of the PEGME arms, displays different solubility in water. We have characterized all of the samples through mass spectrometry and performed elastic and quasielastic light scattering measurements on their solutions. At low molecular mass, star polymers are insoluble in this solvent; at high molecular mass, they have a high solubility; and for intermediate molecular mass, values display interesting colloidal properties. In particular, monodisperse rigid aggregates are present whose size is dependent on pH value. These aggregates arrange in a DLA fractal structure. The supermolecular structure growth is favored by chain flexibility which is modulated by pH changes or by the presence of PEGME coordinating cations.

References and Notes

(1) Likos, C. N.; Lowen, H.; Watzlawek, M.; Abbas, B.; Jucknischke, O.; Allgaier, J.; Richter, D. *Phys. Rev. Lett.* **1998**, *80*, 4450.
(2) von Ferber, C.; Jusufi, A.; Watzlawek, M.; Likos, C. N.; Lowen, H. *Phys. Rev. E* **2000**, *62*, 6949.
(3) Watzlawek, M.; Likos, C. N.; Lowen, H. *Phys. Rev. Lett.* **1999**, *82*, 5289.
(4) Grest, G. S.; Fetters, L. J.; Huang, J. S.; Richter, D. *Adv. Chem. Phys.* **1996**, *XCIV*, 67.
(5) Roovers, J.; Zhou, L.; Toporowski, p. M.; van der Zwan, M.; Iatrou, H.; Hadjichristidis, N. *Macromolecules* **1993**, *26*, 4324.
(6) Likos, C. N.; Lowen, H.; Poppe, A.; Willner, L.; Roovers, J.; Cubitt, B.; Richter, D. *Phys. Rev. E* **1998**, *58*, 6299.
(7) Micali, N.; Villari, V. unpublished results.
(8) Priola, S. A.; Raines, A.; Caughey, W. S. *Science* **2000**, *1287*, 1503.
(9) Caughey, W. S.; Raymond, L. D.; Horiuchi, M.; Caughey, B. *Proc. Natl. Acad. Sci. U.S.A.* **1998**, *95*, 12117.
(10) Ono, N.; Bouhauchi, M.; Maruyama, K. *Tetrahedron Lett.* **1992**, *33*, 1629.
(11) Brunnel, H.; Maiterth, F.; Treittinger, B. *Chem. Ber.* **1994**, *127*, 2141.
(12) Marzilli, D. G. *New J. Chem.* **1990**, *14*, 409.
(13) Little, R. G.; Anton, J. A.; Loach, P. A.; Ibers, J. A. *J. Heterocycl. Chem.* **1975**, *12*, 343.
(14) Scamporrino, E.; Vitalini, D.; Mineo, P. *Macromolecules* **1997**, *30*, 5285.
(15) Mineo, P.; Scamporrino, E.; Vitalini, D. *Macromol. Rapid Commun.* **2002**, *23*, 681.
(16) Berne, B. J.; Pecora, R. *Dynamic Light Scattering with Application to Chemistry, Biology and Physics*; Wiley, J. Sons: New York, 1976.
(17) Stanley, H. E.; Ostrowsky, N., Eds.; *On Growth and Form*; NATO ASI Series; Martinus Nijhoff Publishers: Dordrecht, 1986.
(18) Mallamace, F.; Micali, N. *Riv. Nuovo Cimento* **1992**, *15*, 1.
(19) Kolb, M.; Herrmann, H. J. *Phys. Rev. Lett.* **1987**, *59*, 454.
(20) Keefer, K. D.; Schaefer, D. W. *Phys. Rev. Lett.* **1986**, *56*, 2376.
(21) Chen, S. H.; Teixeira, J. *Phys. Rev. Lett.* **1986**, *57*, 2583.
(22) Cummins, H. Z. In *Photon Correlation and Light Beating Spectroscopy*; Cummins, H. Z., Pike, E. R., Eds.; Plenum Press: New York, 1974.
(23) Schaefer, D. W.; Han, C. C. In *Dynamic Light Scattering*; Pecora, R., Ed.; Plenum: New York, 1985.
(24) Martin, J. E.; Schaefer, D. W. *Phys. Rev. Lett.* **1984**, *53*, 2457.
(25) Lindsay, H. M.; Klein, R.; Weitz, D. A.; Lin, M. Y.; Meakin, P. *Phys. Rev. A* **1989**, *39*, 3112.
(26) Verwey, E. J.; Overbeek, J. Th. G. *Theory of the Stability of Lyophobic Colloids*; Elsevier: Amsterdam, 1984.
(27) Derjajuin, B. V.; Landau, L. *Acta Phys. Chim. Debricina* **1941**, *14*, 633.
(28) Ottewill, R. H. *Sp. Rep. Chem. Soc. Colloid Sci.* **1973**, *1*, 175.
(29) Hamamaker, H. C. *Physica* **1937**, *4*, 1058.
(30) Chandrasekhar, S. *Rev. Mod. Phys.* **1943**, *15*, 1.
(31) Warren, P. B. *Il Nuovo Cimento* **1994**, *16D*, 1231.
(32) Mallamace, F.; Monsu'Scolaro, L.; Romeo, A.; Micali, N. *Phys. Rev. Lett.* **1999**, *82*, 3480.
(33) Mallamace, F.; Micali, N.; Trusso, S.; Monsu'Scolaro, L.; Romeo, A.; Terracina, A.; Pasternack, R. F. *Phys Rev. Lett.* **1996**, *76*, 4741. Pasternack, R. F.; Giannetto, A.; Pagano, P.; Gibbs, E. J. *J. Am. Chem. Soc.* **1991**, *113*, 7799.
(34) Micali, N.; Mallamace, F.; Romeo, A.; Purrello, R.; Monsu'Scolaro, L.; *J. Phys. Chem. B* **2000**, *104*, 5897.
(35) Meakin, P.; Vicsek, T. *Phys. Rev. A* **1985**, *32*, 685.
(36) Vicsek, T. *Fractal Growth Phenomena*; World Scientific: Singapore, 1989.
(37) Pusey, P. N. Rarity, J. G.; Klein, R.; Weitz, D. A. *Phys. Rev. Lett.* **1987**, *59*, 2122.
(38) P. Wiltzius, *Phys. Rev. Lett.* **1987**, *58*, 710.
(39) Triolo, A.; Lo Celso, F.; Arrighi, V.; Strunz, P.; Lechner, R. E.; Mastragostino, M.; Passerini, S.; Annis, B. K.; Triolo, R. *Physica A* **2002**, *304*, 308.
(40) Gong, J.; Dadaatsu, I.; Shigeo, G. *Catal. Today* **2001**, *64*, 279.